Research Article

Jiangwei Liu†, Yan Liu†, Jianzhao Huang*, Lei Huang, Pengwei Zhao

Real-time monitoring of contrast-enhanced ultrasound for radio frequency ablation

https://doi.org/10.1515/med-2017-0066
Received August 23, 2017; accepted November 17, 2017

Abstract: Background: This study compared the real-time monitoring effects of conventional ultrasound and contrast-enhanced ultrasound (CEUS) on evaluating radio frequency ablation (RFA) in a living swine liver model. Methodology: Liver RFA was performed on 10 young swine. Conventional ultrasound and CEUS were performed immediately. After the animals were sacrificed, ablation lesions were removed to histopathologically examine the range of the lesions. Ablation completeness based on three methods were compared using histopathology as the gold standard. Results: Forty-three ablation lesions were produced in the animals. The horizontal diameter, vertical diameter and ablation lesion area based on conventional ultrasound were all significantly smaller than those based on the gross sample, but no significant differences existed between the results of the CEUS and the gross sample. Histopathology showed that 30 lesions were incompletely ablated and 13 were completely ablated, while CEUS showed that 28 lesions were incompletely ablated and 15 were completely ablated. Compared with histopathology, CEUS had an accuracy of 81.4%, a sensitivity of 83.3%, and a specificity of 76.9%. No significant difference in ablation completeness judgment between CEUS and histopathology was observed. Conclusion: CEUS provides a real-time radiological foundation for evaluating RFA lesion ranges and completeness in a living swine liver model.

Keywords: liver cancer; conventional ultrasound; ablation technique; animal experiment

***Corresponding author: Jianzhao Huang**, Department of Hepatobiliary Surgery, Guizhou Provincial People's Hospital, Guizhou 550002, China; E-mail: huangjzgz@126.com
Jiangwei Liu, Yan Liu, Lei Huang, Pengwei Zhao, Department of Hepatobiliary Surgery, Guizhou Provincial People's Hospital, Guizhou 550002, China
†These authors contribute equally to this work.

1 Introduction

As a minimally invasive treatment method, radio frequency ablation (RFA) has been successfully used to treat lung cancer, kidney neoplasms, breast nodules, and thyroid nodules [1-5]. Liver cancer is a common challenging condition in clinical practice and has an incidence and mortality ranking fourth and third among all malignancies, respectively [6]. In recent years, the application of RFA to treat liver cancer has received increasing attention from scholars and surgeons [7-9].

The key to successful RFA is the complete elimination of tumor tissue with the simultaneous minimization of damage to surrounding normal tissues [10]. However, in practice, RFA cannot guarantee complete necrosis of the tumor lesion after a single treatment. Consequently, residual tumor and disease relapse remain great challenges to RFA [10]. For this reason, the timely identification of ablation lesions after RFA and the detection of residual tumor are important in the treatment effectiveness and prognosis judgment.

Currently, the methods used for identifying post-RFA ablation ranges mainly include ultrasound, computed tomography (CT), and magnetic resonance imaging (MRI). In China, CT enhancement is considered the gold standard for judging the curative effects of RFA [11]. However, due to lacking intraoperative real-time guidance, radiation injury and possible contrast agent hypersensitivity, CT and MRI have poor applicability during operations and are therefore not suitable for evaluating early-stage curative effects after RFA. Advantages of ultrasound techniques include real-time guidance, low costs, easy carrying, no radiation and long-term follow-up, thus making ultrasound the preferred method for thermal range evaluation [12, 13]. However, conventional ultrasound has its drawbacks: it is difficult to evaluate ablation ranges of liver cancer that contain isoechoic nodules with fuzzy boundaries, are located at an air interface, or present irregular shapes [14]. As a new technique that has developed rapidly in recent years, contrast-enhanced ultrasound (CEUS) can

effectively overcome the deficiency of conventional ultrasound in evaluating ablation ranges. Using a canine model to investigate the feasibility of using CEUS guidance for the RFA of whole prostates, Liu et al. found no significant differences in thermal lesion size between CEUS and pathological findings [15], implying that CEUS can successfully guide the RFA of the entire prostate [16]. Nevertheless, the application of CEUS for monitoring the RFA of the liver has been rarely reported. Wu et al. used a rat liver model to investigate the monitoring effects of CEUS on RFA, concluding that CEUS may serve as an accurate tool for monitoring the effects of RFA and quantifying the size of thermal damage after RFA [17]. Considering the great differences in the size and other hepatic histological characteristics of rat and human livers and the wide application prospects of RFA in the treatment of cancer, liver models of other animals need to be explored. Because swine (or ox) liver is histologically similar to that of humans, it is often used as an animal tissue model for RFA [18-20]. However, since most previous studies were conducted in vitro, the obtained results may be different from those obtained in living organisms [21].

Based on the aforementioned points, we explored the real-time values of conventional ultrasound and CEUS for judging RFA ablation ranges and completeness in living swine between April and August 2016, which may provide useful data for the ultrasound-guided RFA of liver cancer in the clinic.

2 Materials and methods

2.1 Animals

Ten healthy, young swine (40-45 kg, 6-12 months old) of both genders (6 males and 4 females) were randomly selected and purchased from the Institute of Medical Laboratory Animals at Guiyang College of Traditional Chinese Medicine, Guiyang, China. The animals were not allowed to feed or drink 8h before conventional ultrasound-guided RFA. The flowchart of the experimental design of this study is illustrated in Figure 1.

The surgical procedures were approved by the Animal Ethics Committee of Guizhou Provincial People's Hospital.

2.2 RFA

The animals were anesthetized intramuscularly with pentobarbital sodium (4-6 mg/kg) and Lumianning (2.5-5 mg/kg). Conventional ultrasound was performed to determine the liver area for RFA, and large hepatic vessels were avoided [12]. Under B-scan ultrasonography guidance, the radiofrequency needle was guided percutaneously to the RFA area, and a multipolar needle was then spread. After the tips of the needles reached the target sites, the radiofrequency generator (RITA MODELF; discharge rate, 460 kHz; AngioDynamic, USA) was started.

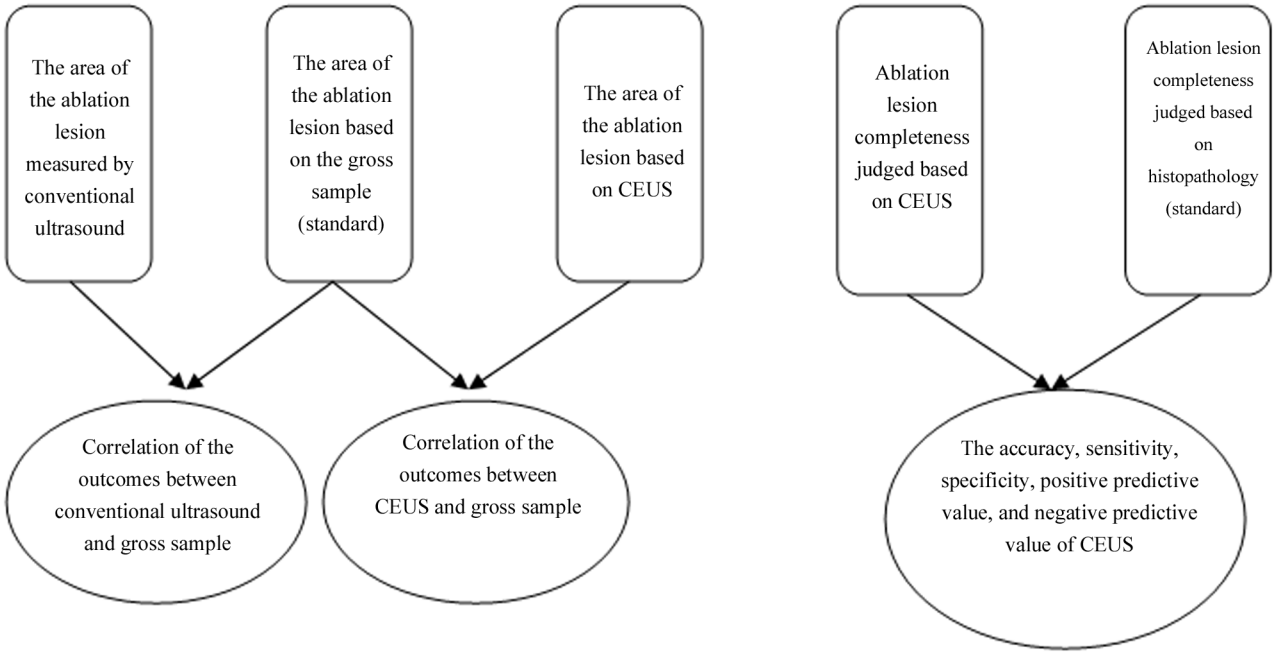

Figure 1. Flowchart of the experimental design of this study.

A temperature of 105 °C, a power of 150 W, and a treatment duration of 5.5 min were used. When the temperatures of all the electrodes reached 105 °C, time was counted. Because surgical ablation and RFA have similar affects on liver tumors ≤ 3 cm [22], 3 cm was designated for RFA in this study. After treatment, the electrode needle was withdrawn slowly to avoid hemorrhage. Then, RFA (≤ 3 cm) was performed repeatedly in the normal liver region for each swine, and 3-5 lesions were produced in each animal.

2.3 Ablation effect observation

2.3.1 Conventional ultrasound

After RFA, conventional ultrasound was performed immediately to scan the ablation lesion range. The maximal cross section was selected, and the left-right and vertical diameters were measured.

2.3.2 CEUS

After conventional ultrasound examination, CEUS (SonoVue; Bracco lmaging B.V., Switzerland) was performed immediately. The optimal location and maximal cross section were selected according to conventional ultrasound. Approximately 2.4 mL of acoustic contrast agent (diluted with 5 mL of physiological saline in advance) was injected using the intravenous bolus method, and the injection site was then rinsed with 5 mL of physiological saline. The dynamic images were taken consecutively within 3-5 min and recorded on hard disks, and the maximal cross section during the CEUS arterial phase was selected. The horizontal and vertical diameters of the section were then measured, and ablation completeness was evaluated according to the following standards: complete ablation, no enhancement at any phase; incomplete ablation, hyperenhancement inside or around the ablation lesion at the arterial phase; and hypo- or non-enhancement in the portal and delayed phases.

2.3.3 Gross sampling and pathological observation

After ultrasound examination, the animals were sacrificed. Hepatic lobes containing the ablation lesions were removed. The incisal section were kept consistent with the image cross-section as much as possible, and horizontal and vertical diameters were measured. Gross samples were fixed with 4% formalin, and tissue sections were marked at intervals of 0.4 cm and then embedded. Hematoxylin-eosin staining was performed for histopathological observation. Ablation completeness was based on the following criteria: complete ablation, without normal hepatic residual cells within the ablation lesion; incomplete ablation, with residual hepatic cells. The data are presented as the average of three experiments, and ablation lesion areas were calculated using the elliptic formula [12].

2.4 Statistical analysis

Data were processed with SPSS17.0 software, and measurement data are presented as the means ± standard deviation ($\bar{x} \pm s$). One-factor analysis of variance was used to compare ablation lesion ranges among the three methods, and *t* tests were performed for pairwise comparisons. Correlation analyses were performed using Pearson's method, and r>0.8 was considered a good correlation. The McNemar test was used for determining the consistency between ablation completeness based on CEUS and that based on pathological observation. P<0.05 was considered statistically significant.

3 Results

Using measurement values of the gross sample and histopathological observations as the gold standard, 43 lesions were produced in the 10 living swine after RFA. No significant differences in the size and number of lesions were observed between the genders (Table 1).

The representative images of CU, CEUS, and the histological observation of liver lesions are shown in Figure 2. The horizontal and vertical diameters and ablation area based on conventional ultrasound were all smaller than those based on the gross sample (all P<0.05; Table 2). In contrast, the values obtained from CEUS did not show significant differences compared with those obtained from the gross sample (all P>0.05). The raw measurement data are summarized in Supplementary Table 1. The correlation coefficients of horizontal diameter, vertical diameter, and ablation lesion area based on conventional ultrasound compared with those based on the gross sample were 0.977, 0.943, and 0.956, respectively (all P<0.05), whereas those based on CEUS were 0.949, 0.958, and 0.919, respectively (all P<0.05; Table 3).

According to histopathological observation, among the 43-ablation lesions, 30 were complete and 13 were

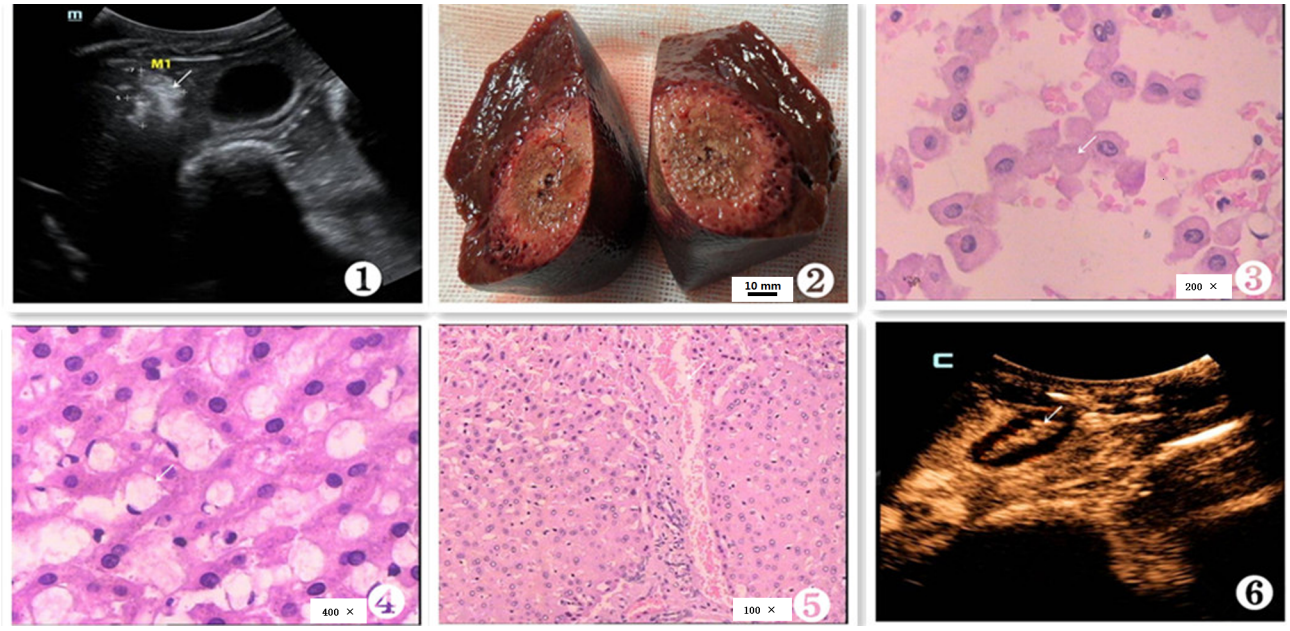

Figure 2. Representative images of conventional ultrasound (CU), contrast-enhanced ultrasound (CEUS), and the histologically stained liver lesions. 1: The ablation lesion presents an inhomogeneous hyperechoic mass according to CU (indicated by the white arrow); 2: the gross image of the radio frequency ablation (RFA) lesions of the swine livers in vitro; 3: coagulative necrotic hepatocytes inside a complete ablation lesion (indicated by the white arrow); 4: edema (indicated by the white arrow) and pyknosis of hepatocytes inside an incomplete ablation lesion; 5: reactive hyperemia zone between the ablation lesion and normal hepatic tissue (indicated by the white arrow); and 6: mass-like echo enhancement of an incomplete ablation lesion in the arterial phase according to CEUS (indicated by the white arrow).

Table 1. Comparisons of the areas and number of ablation lesions between genders based on the three different measurement methods.

	Male (n=6)	Female (n=4)	P value
Area (cm^2)			
Conventional	7.35 ± 1.58	7.32 ± 1.56	0.15
CEUS	7.61 ± 1.62	7.58 ± 1.60	0.18
Gross sample	7.63 ± 1.59	7.62 ± 1.58	0.12
Amount	24	19	0.41

Table 2. Measurement values of the lesion ranges based on three methods ($\bar{x}$ ±s)

Method	Horizontal diameter (cm)	Vertical diameter (cm)	Area (cm^2)
Conventional	3.27 ± 0.51*	2.81 ± 0.50*	7.20 ± 1.59*
CEUS	3.36 ± 0.57	2.90 ± 0.55	7.60 ± 1.65
Gross sample	3.40 ± 0.60	2.88 ± 0.55	7.66 ± 1.79

*P<0.05 vs. the gross sample. CEUS, contrast-enhanced ultrasound.

Table 3. Pearson correlation analyses of the ablation lesion areas as measured by the three methods.

Method	Horizontal diameter (cm)	Vertical diameter (cm)	Area (cm^2)
Gross/conventional	0.977	0.943	0.956
Gross/CEUS	0.949	0.958	0.919
Conventional/CEUS	0.922	0.907	0.853

Gross, gross sample. CEUS, contrast-enhanced ultrasound.

Table 4. Comparison of the judgment of ablation lesion completeness between contrast-enhanced ultrasound (CEUS) and histopathology.

	CEUS	Histopathology
Residual	28	30
Non-residual	15	13
Total	43	43

incomplete. According to CEUS, 28 ablation lesions were incomplete and 15 were complete. The accuracy, sensitivity, specificity, positive predictive value, negative predictive value, misdiagnosis rate, positive likelihood ratio, and negative likelihood ratio of CEUS in ablation lesion judgment were 81.4%, 83.3%, 76.9%, 89.3%, 66.7%, 16.7%, 3.61, and 0.22, respectively. The CEUS results of ablation completeness judgments were basically consistent with those of histopathological observation (P=0.727). These results are summarized in Table 4.

4 Discussion

In this study, we compared ablation range measurements using conventional ultrasound, CEUS, and histopathological observation and analyzed the value of CEUS in judging ablation completeness using histopathological results as standards.

By using normal swine livers as the subjects, we compared the horizontal diameters, vertical diameters and maximal cross section areas of ablation lesions based on conventional ultrasound with those based on the gross sample. Significant differences were observed between these two methods; furthermore, linear correlation analysis showed a high correlation between the results obtained from the two methods. Correa-Gallego et al. performed hepatic microwave ablation for living swine and evaluated the ablation lesion range immediately, 5 min and 10 min after treatment. Using measured values obtained from the post-operative gross sample and cellular histopathology as the standards, conventional ultrasound failed to clearly reflect the actual ablation range, and the measured range decreased with time delay compared with the standard value, which was consistent with our results [11]. Presumably, liver tissue may present isoechoes, or uneven hyperechoic masses, after RFA because of different degrees of ablation. During RFA, liver tissue is heated and carbonized to produce air, and when conventional ultrasound is performed, ultrasonic cavitation occurs, thus increasing the changeability of air. For this reason, hyperechoic masses in ablation lesions often cause echo enhancement, which can even exceed the ablation range. Therefore, errors often occur when measuring real-time ablation ranges in living swine livers after RFA based on conventional ultrasound due to interfering factors, such as air [14]. In contrast, our study showed no significant differences in ablation lesion ranges between CEUS and the gross sample, and linear correlation analysis showed high correlations between the results of CEUS and those based on the gross sample. Therefore, CEUS is applicable for the real-time judgment of ablation range in living swine livers after RFA and can offer a reliable radiological foundation in this respect.

Whether a lesion is ablated completely based on CEUS is determined by whether the ablation lesion is enhanced, i.e., whether the acoustic contrast agent enters the ablation lesion, as the contrast agent cannot enter the ablation lesion due to no blood supply if coagulative necrosis occurs [23]. In this study, eight ablation lesions according to CEUS were not consistent with those based on the gross sample. Among these ablation lesions, five were not enhanced at any phase of CEUS, but residual normal hepatic cells were found based on histological observation, leading to misdiagnosis. The remaining three ablation lesions were incomplete according to CEUS, which showed a narrow strong echo band around the lesion with a width of 1-2 mm. These lesions presented high enhancement at the arterial phase, which remained high or equal at the portal and delayed phases. While no normal hepatic cells were observed histologically, a reactive hyperemia zone was observed. Because reactive hyperemia is a key factor influencing the ablation effect [24], great attention should be paid to the reactive hyperemia zone around the ablation lesion while CEUS is being performed after RFA, based on our results. Hyperemia zones are mostly presented as thin, uniform, morphologically regular high-level echo enhancement bands along ablation lesion margins, while ablation lesion margins of residual normal hepatic cells mostly present nodule-like and irregular high-level echo enhancement masses. Compared with histopathology, CEUS ablation completeness judgement had an accuracy of 81.4%, a sensitivity of 83.3%, and a specificity of 76.9%. No significant differences were observed between CEUS and histopathology according to the McNemar test, indicating that CEUS can provide

a radiological foundation for ablation completeness in living swine livers after RFA.

However, this study has limitations. First, CEUS can be performed immediately after RFA, which is a great advantage compared with the enhanced CT method. While CEUS suggested continuous blood flow in some lesions, presumably caused by residual blood vessels that were closed incompletely, this analysis needs to be confirmed in future studies. Second, the study sample size was relatively small, and long-term follow-ups were not conducted after RFA. In the future, the sample size should be increased, and comparative studies on the outcomes of CEUS, enhanced CT, and histopathology at a late stage should be conducted.

In conclusion, compared with conventional ultrasound, CEUS can more clearly reflect ablation lesion size and more accurately evaluate ablation lesion completeness after RFA for the swine liver model. For patients who need a second round of RFA immediately after the first, CEUS may be a better choice for RFA monitoring and guidance. However, the validity and practicality of these study results remain to be validated in clinical practice.

Conflict of interest: The authors declare no conflicts of interest.

Acknowledgments: This study was supported by the United Foundation of Guizhou Province Science and Technology Committee (No.2014-7016).

References

[1] Widmann G.P., Schullian R., Bale R., Radiofrequency ablation of hepatocellular carcinoma, Wien Med. Wochenschr., 2013, 163, 132-136.

[2] Jahangeer S., Forde P., Soden D., Hinchion J., Review of current thermal ablation treatment for lung cancer and the potential of electrochemotherapy as a means for treatment of lung tumours, Cancer Treat. Rev., 2013, 39, 862-871.

[3] Popovic P., Lukic S., Mijailovic M., Salapura V., Garbajs M., Surlan Popovic K., Percutaneous radiofrequency ablation of small renal cell carcinoma: technique, complications, and outcomes, J. BUON., 2012, 17, 621-626.

[4] Vogl T.J., Farshid P., Naguib N.N., Zangos S., Thermal ablation therapies in patients with breast cancer liver metastases: a review, Eur. Radiol., 2013, 23, 797-804.

[5] Shin J.E., Baek J.H., Lee J.H., Radiofrequency and ethanol ablation for the treatment of recurrent thyroid cancers: current status and challenges, Curr. Opin. Oncol., 2013, 25, 14-19.

[6] Jemal A., Bray F., Center M.M., Ferlay J., Ward E., Forman D., Global cancer statistics, CA Cancer J. Clin., 2011, 61(2), 69-90.

[7] Bruix J., Sherman M., Management of hepatocellular carcinoma: an update, Hepatology, 2011, 53(3), 1020-1022.

[8] Tandon M., Pandey C.K., Myocardial oxidative stress protection with sevoflurane versus propofol, Eur. J. Anaesthesiol., 2012, 29(6), 296-297.

[9] Min J.H., Lee M.W., Rhim H., Choi D., Kim Y.S., Kim Y.J., et al., Radiofrequency ablation for viable hepatocellular carcinoma around retained iodized oil after transcatheter arterial chemoembolization: usefulness of biplane fluoroscopy plus ultrasound guidance, Korean J. Radiol., 2012, 13, 784-794.

[10] Liao J.T., Pan R.J., Liu Y., Guo M.A., Wang Z.M., Zhou L.D., et al., Assessment of short term therapeutic response to radiofrequency ablation by contrast enhanced ultrasound in hepatocellular carcinoma, Chin. J. Basess Clin. General Surg., 2009, 16, 265-268 (in Chinese with an English abstract)

[11] Correa-Gallego C., Karkar A.M., Monette S., Ezell P.C., Jarnagin W.R., Kingham T.P., Intraoperative ultrasound and tissue elastography measurements do not predict the size of hepatic microwave ablations, Acad. Radiol., 2014, 21(1), 72-78.

[12] Liu F., Yu X., Liang P., Cheng Z., Han Z., Dong B., Contrast-enhanced ultrasound-guided microwave ablation for hepatocellular carcinoma inconspicuous on conventional ultrasound, Int. J. Hyperthermia., 2011, 27, 555-562.

[13] Takahashi M., Maruyama H., Ishibashi H., Yoshikawa M., Yokosuka O., Contrast enhanced ultrasound with perflubutane microbubble agent: evaluation of differentiation of hepato-cellular carcinoma, AJR Am. J. Roentgenol., 2011, 196, 123-31.

[14] Jiang Y.X., Liu H., Liu J.B., Zhu Q.L., Sun Q., Chang X.Y., Breast tumor size assessment: comparison of conventional ultrasound and contrast-enhanced ultrasound, Ultrasound Med. Biol., 2007, 33, 1873-1881.

[15] Liu J.B., Merton D.A., Wansaicheong G., Forsberg F., Edmonds P.R., Deng X.D., et al., Contrast enhanced ultrasound for radio frequency ablation of canine prostates: initial results, J. Urol., 2006, 176, 1654-1660.

[16] Liu J.B., Wansaicheong G., Merton D.A., Chiou S.Y., Sun Y., Li K., et al., Canine prostate: contrast-enhanced US-guided radiofrequency ablation with urethral and neurovascular cooling--initial experience, Radiology, 2008, 247, 717-725.

[17] Wu H., Wilkins L.R., Ziats N.P., Haaga J.R., Exner A.A., Real-time monitoring of radiofrequency ablation and postablation assessment: accuracy of contrast-enhanced US in experimental rat liver model, Radiology, 2014, 270, 107-116.

[18] Brace C.L., Laeseke P.F., van der Weide D.W., Lee F.T., Microwave ablation with a triaxial antenna: results in ex vivo bovine liver, IEEE Trans. Microw. Theory Tech., 2005, 53, 215-220.

[19] Yang D., Converse M.C., Mahvi D.M., Webster J.G., Measurement and analysis of tissue temperature during microwave liver ablation, IEEE Trans. Biomed. Eng., 2007, 54, 150-155.

[20] Shi W.Y., Liang P., Zhu Q., Yu X., Shao Q., Lu T., et al., Microwave ablation: results with double 915 MHz antennae in ex vivo bovine livers, Eur. J. Radiol., 2011, 79, 214-217.

[21] Wang Y., Sun Y., Feng L., Gao Y., Ni X., Liang P., Internally cooled antenna for microwave ablation: results in ex vivo and in vivo porcine livers, Eur. J. Radiol., 2008, 67, 357-361.

[22] Minstry of Health of the PRC, Diagnosis and treatment of primary liver cancer (2011), J. Clin. Oncol., 2011, 16, 938 (in Chinese).

[23] Mori K., Fukuda K., Asaoka H., Ueda T., Kunimatsu A., Okamoto Y., et al., Radiofrequency ablation of the liver: determination of ablative margin at MR imaging with impaired clearance of ferucarbotran--feasibility study, Radiology, 2015, 251, 557-565.
[24] Kim Y.S., Rhim H., Cho O.K., Koh B.H., Kim Y., Intrahepatic recurrence after percutaneous radiofrequency ablation of hepatocellular carcinoma: analysis of the pattern and risk factors, Eur. J. Radiol., 2010, 59, 432–441.

Supplemental Material: The online version of this article (DOI: 10.1515/med-2017-00xx) offers supplementary material.